AGU PUBLICATIONS

Geophysical Research Letters

RESEARCH LETTER
10.1002/2016GL071367

Key Points:
- Explosive cyclones over the North Pacific cause strong surface divergence and upward flow reaching 2000 m depth
- Upward flow induces near inertial waves in the ocean and cools the ocean interior by vertical advection
- Stronger explosive cyclone activity amplifies the daily-scale variations of the vertical velocity and temperature in the deep ocean

Supporting Information:
- Supporting Information S1

Correspondence to:
A. Kuwano-Yoshida,
akiray@jamstec.go.jp

Citation:
Kuwano-Yoshida, A., H. Sasaki, and Y. Sasai (2017), Impact of explosive cyclones on the deep ocean in the North Pacific using an eddy-resolving ocean general circulation model, *Geophys. Res. Lett.*, *44*, 320–329, doi:10.1002/2016GL071367.

Received 27 SEP 2016
Accepted 1 DEC 2016
Accepted article online 5 DEC 2016
Published online 12 JAN 2017

Impact of explosive cyclones on the deep ocean in the North Pacific using an eddy-resolving ocean general circulation model

Akira Kuwano-Yoshida[1], Hideharu Sasaki[1], and Yoshikazu Sasai[2]

[1]Application Laboratory, Japan Agency for Marine-Earth Science and Technology, Yokohama, Japan, [2]Research and Development Center for Global Change, Japan Agency for Marine-Earth Science and Technology, Yokosuka, Japan

Abstract The oceanic response to explosive cyclones over the North Pacific in winter is investigated using eddy-resolving 34 year hindcast simulation of a quasi-global ocean. Its response appears as a horizontal divergence of the surface layer above 60 m depth and upward flow that reaches 2000 m depth. A case study of a typical explosive cyclone using hourly outputs from January 2011 shows that the explosive cyclone induces horizontal divergence within the surface-mixed layer and upward flow that reaches 6000 m depths. The flow causes oceanic internal waves and temperature cooling because of the vertical advection in the deep ocean. The interannual variability of explosive cyclone activity in January affects the amplitude of the vertical motion and the daily-scale temperature variations in the deep ocean.

1. Introduction

Explosive cyclones, also referred to as "bomb cyclones," are extratropical cyclones that present central sea-level pressure deepening that exceeds 24 hPa d^{-1} normalized by the ratio between the sine of a given latitude (60° or 45°) and the sine of the cyclone center latitude. These cyclones usually develop associated with strong winds over the ocean [*Sanders and Gyakum*, 1980], and they are especially concentrated over sea surface temperature (SST) fronts associated with western boundary currents, such as the Kuroshio and its extension, the Gulf Stream, and the Agulhas return current. The concentrations appear in the atmospheric "storm track." The large heat flux from the SST fronts works an important role to maintain the storm track through atmospheric baroclinicity restoration [*Nakamura et al.*, 2004; *Minobe et al.*, 2008]. Recently, *Kuwano-Yoshida and Minobe* [2016] suggested that evaporation from the Kuroshio concentrates explosive cyclones in the west of North Pacific (NP).

The storm track is one of the energy sources of oceanic internal gravity waves, especially near-inertial waves (NIWs). *Alford et al.* [2016] reported that midlatitude storms provide the wind to generate NIWs. *Komori et al.* [2008] demonstrated NIWs in the deep ocean using a coupled general circulation model, whose horizontal resolutions are 50 km in the atmosphere and 0.25° in the ocean. *Furuichi et al.* [2008] estimated the wind-induced internal wave energy using an eddy-resolving ocean general circulation model (OGCM) and showed that the NIWs appear in the deep ocean under the atmospheric storm track in the NP, which is much deeper than the North Atlantic (Figure 1).

However, a general consensus has not been reached on the oceanic response to individual explosive cyclones. In particular, few studies have focused on the influence of explosive cyclones on the deep ocean. *Ren et al.* [2004] and *Yao et al.* [2008] conducted case studies to investigate the oceanic responses at depths shallower than 1000 m to extratropical cyclones developing over the North Atlantic using regional atmospheric-ocean coupled models. These authors suggested that the SST cooling is small because of the deep oceanic mixed layer in winter, although the storm-induced ocean current can be large.

The purpose of the present study is to clarify the oceanic responses of the entire layer to individual explosive cyclones and the interannual variability of their activity in the NP using several decades of eddy-resolving OGCM simulation output forced by atmospheric reanalysis.

2. Data and Methods

We use eddy-resolving hindcast simulation data for a quasi-global ocean from the OGCM for the Earth Simulator (OFES) [*Sasaki et al.*, 2008]. The horizontal resolution is 0.1° × 0.1° between 75°S and 75°N in latitude.

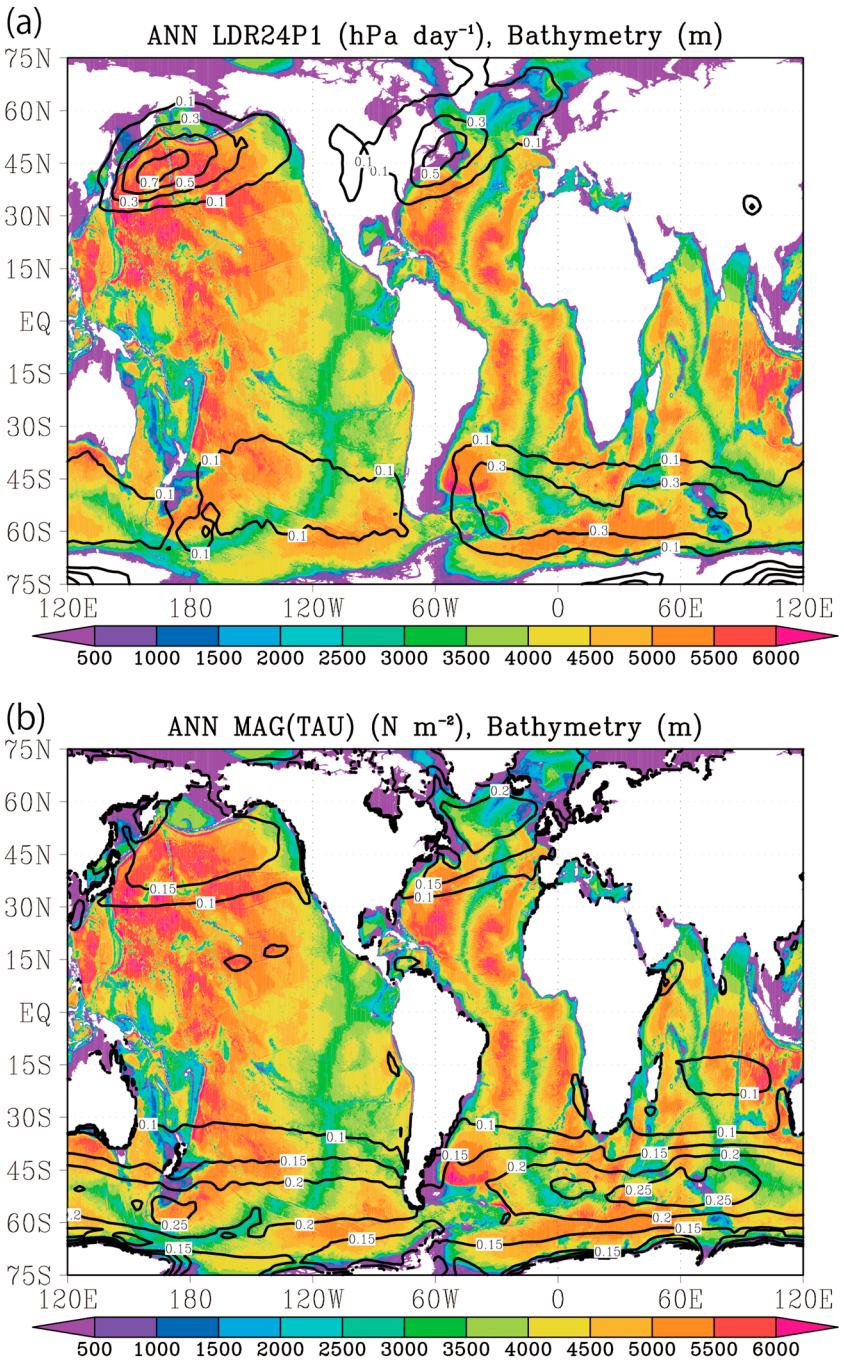

Figure 1. Annual means of (a) LDR24P1 (hPa d^{-1}, contour from 0.1) and (b) magnitude of the wind stress (N m^{-2}, contour from 0.1) with the bathymetry used in the OFES (m, shaded).

The vertical resolution varies from 5 m at the surface to 330 m at the maximum depth of 6065 m over 54 levels. The model topography is based on a 1/30° bathymetry data set provided by the Ocean Circulation and Climate Advanced Modelling (OCCAM) project of the National Oceanography Centre, Southampton. The simulation starts on 1 January 1950. The data are forced by the daily mean wind stress and net shortwave fluxes of the National Centers for Environmental Prediction (NCEP)/National Center for Atmospheric Research (NCAR) reanalysis with 2.5° horizontal resolutions [*Kalnay et al.*, 1996]. The other heat fluxes are calculated using a bulk method [*Rosati and Miyakoda*, 1988] and the NCEP/NCAR reanalysis. Note that wind stress does not depend on the ocean current velocity and the atmospheric pressure is excluded in the forcing. Thus, the

explosive pressure deepening does not force the ocean model directly. The 50 year climatological integration with the climate forcing [*Masumoto et al.*, 2004] is used as the initial state. Because the snapshot data are stored every 3 days starting on 1 January 1980, we analyze from January 1980 to December 2013.

Explosive cyclones are extracted using the local deepening rate (LDR) introduced by *Kuwano-Yoshida* [2014]:

$$\mathrm{LDR} = -\frac{\partial p_{\mathrm{sfc}}}{\partial t}\left|\frac{\sin 60^\circ}{\sin\theta}\right|, \tag{1}$$

where p_{sfc} is the surface pressure, t is the time, and θ is the latitude. In the present study, the 24 h backward difference, LDR24, is calculated using the daily mean surface pressure of the NCEP/NCAR reanalysis consistent with the forcing data:

$$\mathrm{LDR24} = -\frac{p_{\mathrm{sfc}}(t) - p_{\mathrm{sfc}}(t-24h)}{24}\left|\frac{\sin 60^\circ}{\sin\theta}\right|, \tag{2}$$

Monthly explosive cyclone activity is estimated using the monthly means of LDR24 ≥ 1 hPa h^{-1} (LDR24P1):

$$\begin{aligned} \mathrm{LDR24P1} &= \frac{1}{n}\sum_{i=1}^{n}\sigma_1(t=i) \\ \sigma_1 &= \begin{cases} \mathrm{LDR24}, & \text{if LDR24}\geq 1\ \text{hPa h}^{-1} \\ 0, & \text{otherwise} \end{cases}, \end{aligned} \tag{3}$$

where n is the number of averaged time steps. Because the explosive cyclones usually develop in winter [*Yoshida and Asuma*, 2004], we analyze the explosive cyclones between December and March when they are active over the NP.

Figure 1 shows the climatologies of the annual mean LDR24P1 and the wind stress magnitude with bathymetry used in the OFES. The explosive cyclone activity in the NP is the largest in the world (Figure 1a), although the wind stress magnitude is smaller than in other storm tracks over the North Atlantic and the Southern Indian Oceans (Figure 1b). The bathymetry of the NP under the large explosive cyclone activity is deeper than 5500 m, which is the deepest among the three oceans.

To analyze the oceanic response to the individual explosive cyclones in the NP, explosive deepening events with LDR24 ≥ 1 hPa h^{-1} extracted at the maximum annual mean LDR24P1 at 165°E and 42.5°N are composited. Because the extraction is based on LDR24 with a 3 day interval and explosive cyclones usually stay for less than a day at the point, the composited 76 samples do not include duplication events. The statistical significance of the composite difference from the prior 3 day lag composite is estimated by the Student's t test.

3. Oceanic Responses Under Explosive Deepening Events

Figure 2 shows the composites of the LDR24, wind stress, wind stress curl, and surface oceanic current. The wind stress curl maximum overlaps with the LDR24 maximum and spreads northeastward (Figure 2a). The difference of the wind stress curl within a 3 day interval is statistically significant near the cyclone center (Figure 2c), whereas the wind stress magnitude shows a broader significant area, with two peaks south and north of the LDR24 maximum (Figure 2b). The wind stress forces the cyclonic surface oceanic current (Figure 2d). In particular, the northward current northeast of the LDR24 maximum is statistically significant.

The current change induces horizontal divergence of the surface layer northeast of the LDR24 maximum (Figure 3a). However, the distribution is noisy, especially south of the cyclone center, where oceanic eddies are active along the Kuroshio Extension and the Oyashio [*Sasaki et al.*, 2008]. To filter out the divergence associated with oceanic eddies, the composites are horizontally smoothed using the 1-2-1 filter with a 40 times for 0.1° grid, which retains the atmospheric forcing scale of 2.5° (e.g., Figures 4b and 4d). The smoothed composite shows a clear divergence response. A divergence zone appears between 39°N and 48°N under the wind stress curl maximum (Figure 3b), and the significant area extends to the west of the cyclone center. The divergence is vertically confined for layers shallower than 60 m depth (Figure 3c).

The surface divergence induces upward flow in the deep ocean. The composite of the vertical velocity at a depth of 200 m shows that the upward flow overlaps just under the surface divergence (Figure 3d). At deeper

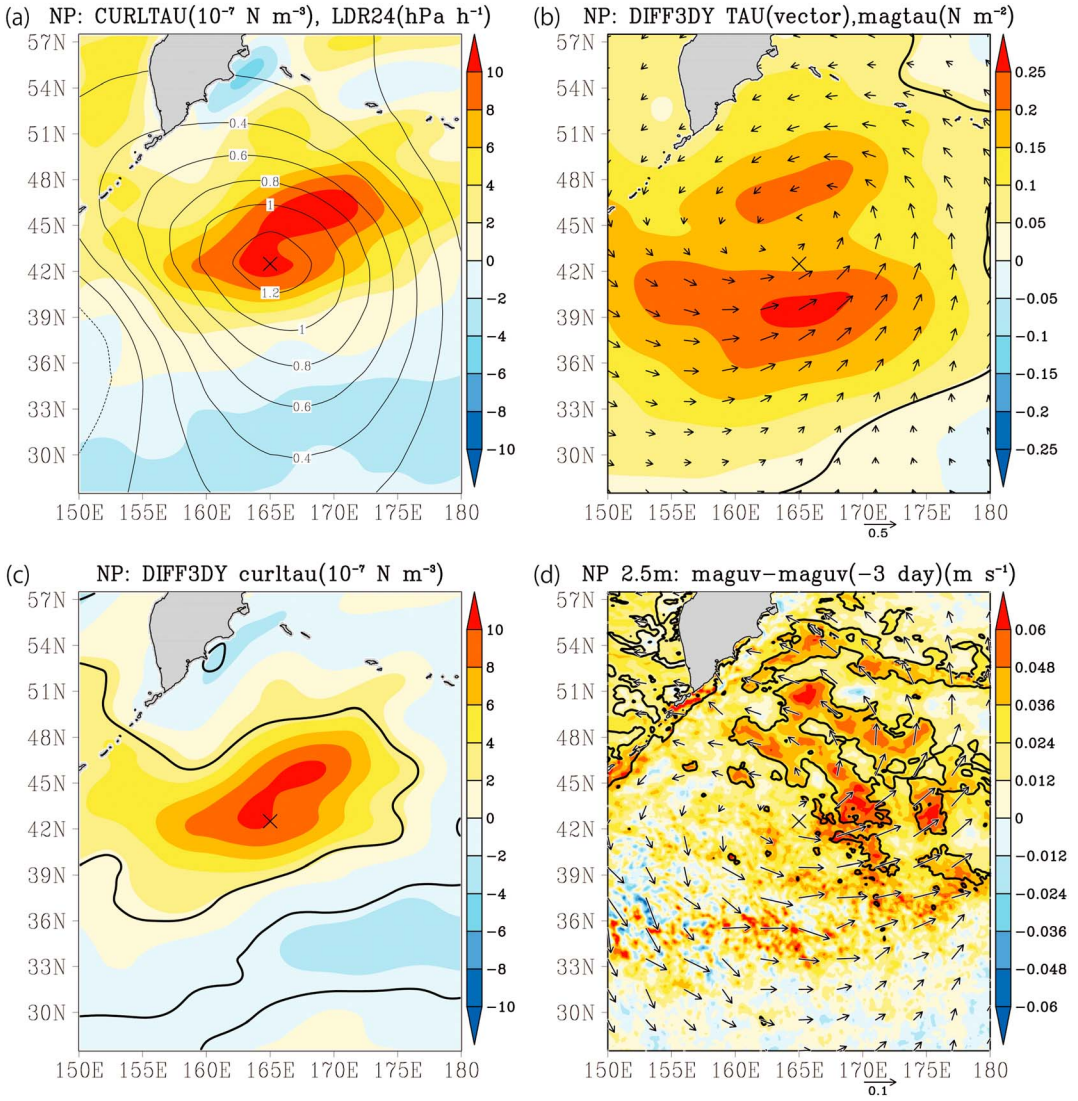

Figure 2. Composites for the explosive deepening event at 165°E, 42.5°N (cross mark). (a) Wind stress curl (10^{-7} N m^{-3}, shaded) and LDR24 (hPa h^{-1}, contour), (b) wind stress (N m^{-2}, vector) and its magnitude (N m^{-2}, shaded), (c) difference of the wind stress curl from 3 days before (10^{-7} N m^{-3}, shaded), and (d) same as in Figure 2c but for ocean currents of 2.5 m depth (m s^{-1}, vector) and the magnitude (m s^{-1}, shaded) from 3 days before. Black contours in Figures 2b–2d represent the 95% confidence level.

layers, the upward flow concentrates along the Hawaiian-Emperor seamount chain (Figure 3e). The vertical cross section shows that a broad upwelling appears from the surface to a depth of 1000 m and the sharp upwelling penetrates even to 4000 m along the seamount chain (Figure 3f). Horizontal currents show cyclonic anomaly under 1500 m depth (Figures 3g–3i). The interaction between the circulation and the seamount chain seems to induce the upward flow concentration.

4. Case Study of an Explosive Cyclone in January 2011

The composite analysis using 3 day interval data suggests that explosive cyclones induce surface divergence and upward flows that penetrate into the deep ocean. However, the temporal resolutions are too sparse to reveal the oceanic response to explosive cyclones because the time scale of explosive cyclones is shorter than 3 days. Therefore, to describe the evolution of the oceanic response, we analyze a typical case of an explosive cyclone using outputs in 1-hourly intervals from the OFES from 1 to 31 January 2011, which were recalculated with the same forcing as used by *Tanaka et al.* [2015].

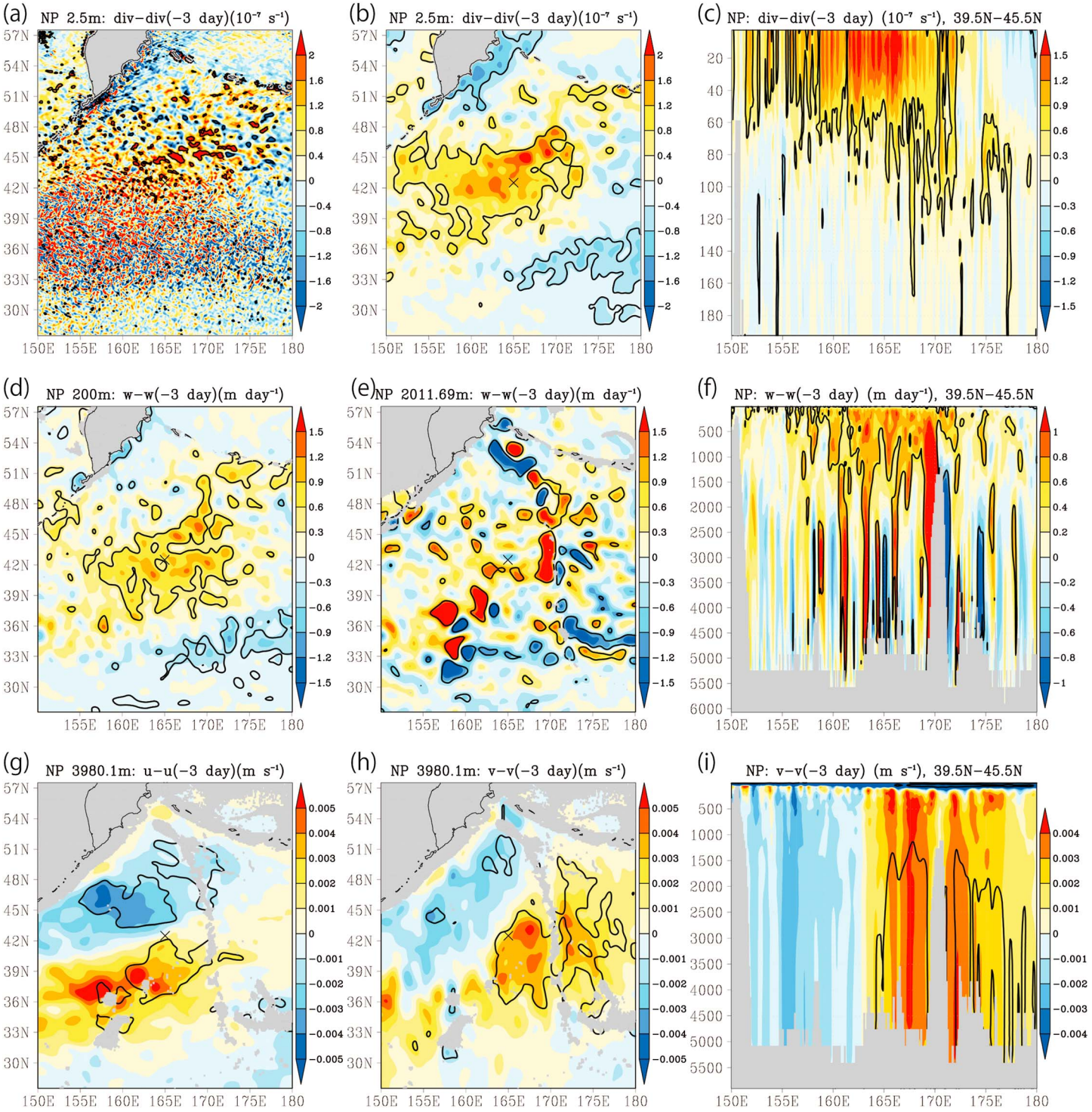

Figure 3. Composite differences for the explosive deepening events from 3 days prior. (a) Horizontal divergence of the ocean current at 2.5 m depth, (b) same as in Figure 3a but horizontally smoothed, (c) vertical-zonal cross section of the horizontal divergence averaged between 39.5°N and 45.5°N (10^{-7} s^{-1}, shaded), (d) vertical velocity at 200 m depth, (e) at 2011.69 m, (f) vertical-zonal cross section (m d^{-1}, shaded), (g) zonal and (h) meridional current at 3980.1 m, and (i) its vertical-zonal cross section (m s^{-1}, shaded). Black contours represent a 95% confidence level.

An explosive cyclone developed over the NP between 16 and 17 January 2011. The wind stress curl rapidly strengthens with the cyclone development starting at 12 UTC on 15 January and peaks at 12 UTC on 17 January (Figure 4a). As the wind stress changes, surface divergence is induced under the wind stress curl

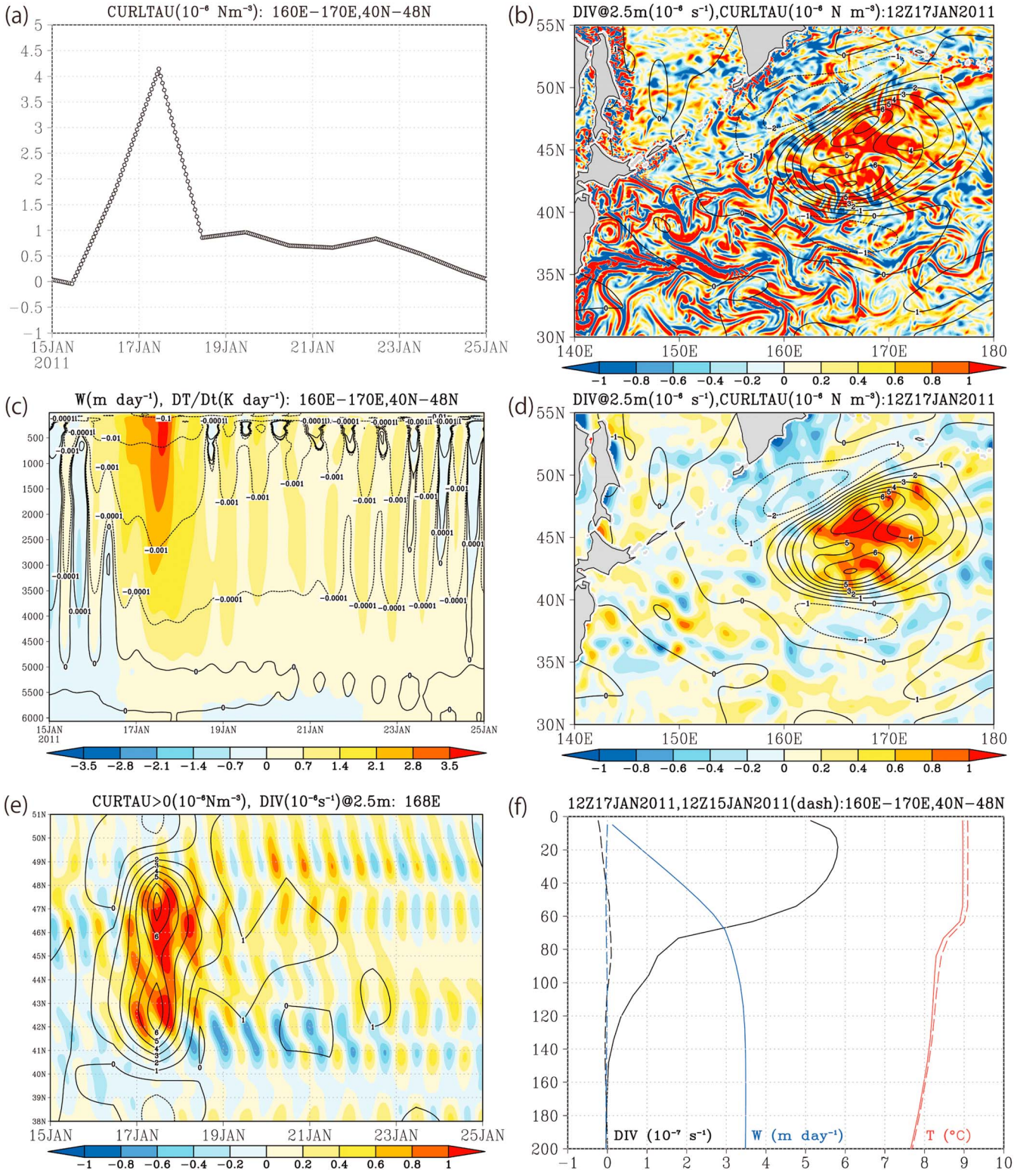

Figure 4. (a) Time series of the wind stress curl from 00 UTC on 15 January to 00 UTC on 25 January 2011 (10^{-6} N m^{-3}). (b) Horizontal divergence of the ocean current at 2.5 m depth (10^{-6} s^{-1}, shaded) and the wind stress curl (10^{-6} N m^{-3}, contour) at 12 UTC on 17 January 2011. (c) Vertical-time cross section of the vertical velocity (m d^{-1}, shaded) and temperature tendency (K d^{-1}, contour, C. I: 0.1, 0.01, 0.001, and 0.0001). (d) Same as in Figure 4a but horizontally smoothed. (e) Latitude-time section of the wind stress curl (10^{-6} N m^{-3}, contour) and horizontal divergence of the ocean current at 2.5 m depth along 168°E with horizontal smoothing (10^{-6} s^{-1}, shaded). (f) Vertical profiles of the horizontal divergence (10^{-7} s^{-1}, black), vertical velocity (m d^{-1}, blue) and temperature (K, red) at 12 UTC on 17 January 2011 (solid lines) and 12 UTC on 15 January 2011 (broken lines). Figures 4a, 4c, and 4d are averaged between 160°E and 170°E and 40°N and 48°N.

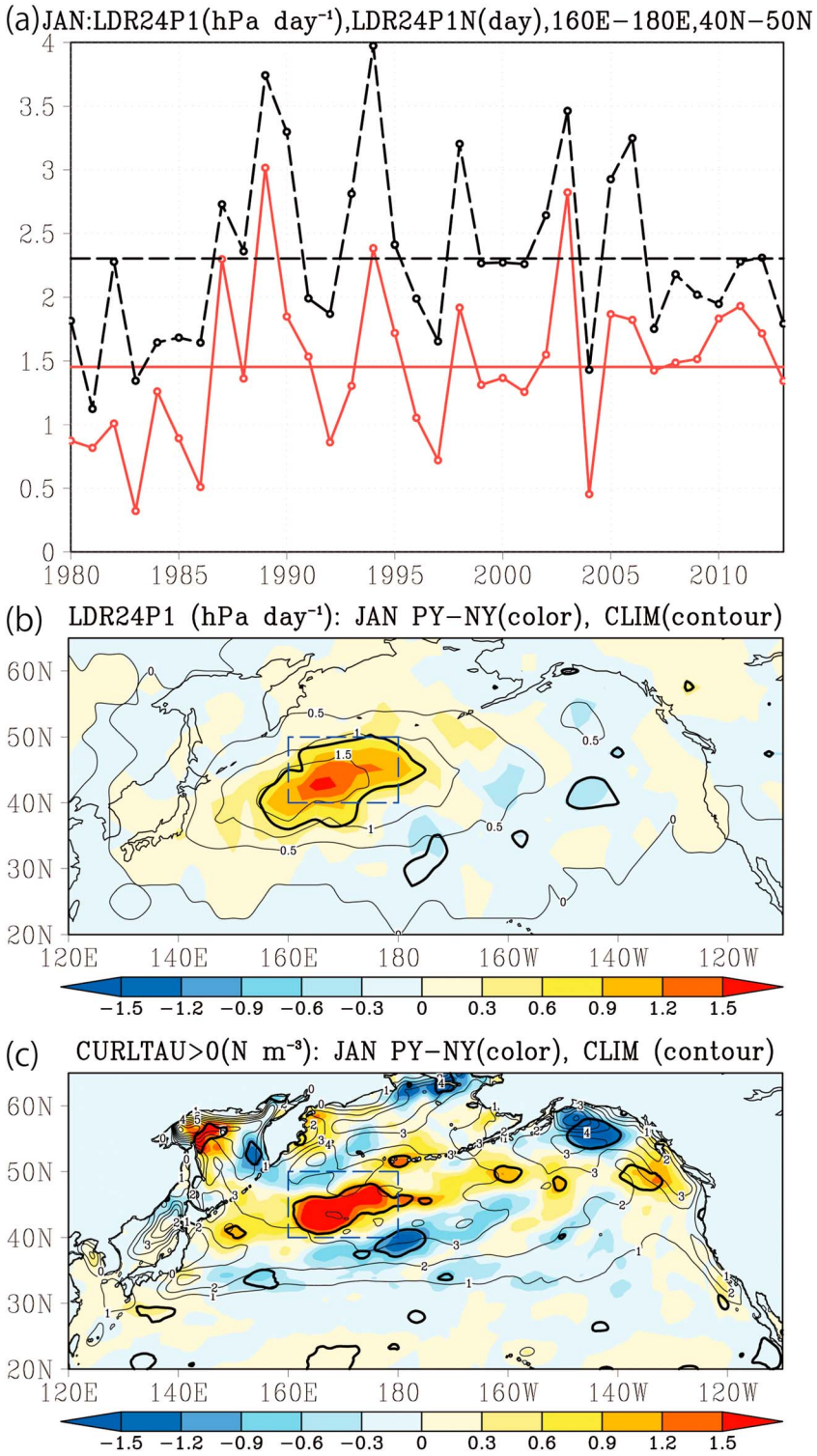

Figure 5. (a) Interannual time series of the LDR24P1 (red, hPa d^{-1}) and the accumulated time with LDR24 ≥ 1 hPa h^{-1} (black, day) in January averaged between 160°E and 180° and 40°N and 50°N (rectangles in Figures 5b and 5c); (b) composite difference of the LDR24P1 in January between PY and NY (hPa d^{-1}, shaded) and the LDR24P1 climatology in January (hPa d^{-1}, contour); and (c) same as in Figure 5b but for the positive wind stress curl (N m^{-3}). Bold contours in Figures 5b and 5c show the 95% confidence level.

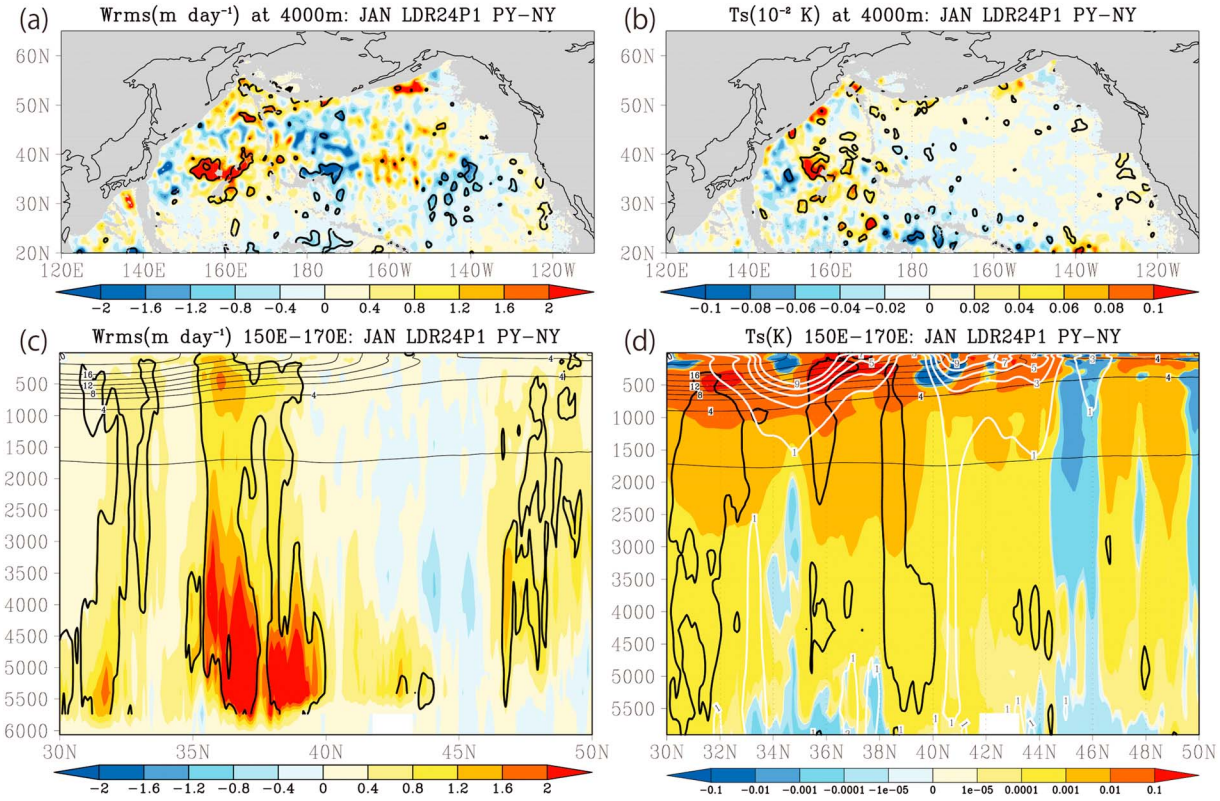

Figure 6. Composite differences between the PY and NY for the RMS in January for the (a) vertical velocity (m d^{-1}, shaded); (b) the temperature standard deviation from the monthly mean (10^{-2} K, shaded) at a depth of 4000 m; and (c and d) vertical-meridional cross sections averaged between 150°E and 170°E. Bold black contours show the 95% confidence level. The thin black contour in Figures 6c and 6d represents the temperature climatology (°C). The white contour in Figure 6d is the climatological zonal velocity in January (10^{-2} m s^{-1}). The composites in Figures 6a and 6b are smoothed horizontally, which is similar to Figure 3b.

maximum at 12 UTC on 17 January and upward flow develops in the deep ocean to depths of 5500 m (Figures 4b–4d). The temperature tendency, which is the temperature change within the prior 1 h, indicates cooling by the upward flow from the surface to 5000 m. After the rapid change of the wind stress curl at 12 UTC on 18 January, the vertical velocity and temperature tendency oscillate. The divergence is induced when the wind stress curl rapidly changes and oscillates with near-inertial oscillation period about 17 h at 43°N and 16 h at 47°N (Figure 4e). The results suggest that NIWs are induced by the explosive cyclone. The surface divergence is confined to depths of 60 m and above (Figure 4f). The depth of divergence is consistent with the mixed layer depth estimated from the temperature profile, although the upward flow is induced under the mixed layer.

5. Response to Interannual Variation of Explosive Cyclones

Explosive cyclone activity shows large interannual variations [*Gyakum et al.*, 1989]. *Dippe et al.* [2015] suggested that the wind power input to the near-inertial motion in the North Atlantic is modified by storm path changes associated with the North Atlantic Oscillation. Figure 5a shows the interannual time series of the LDR24P1 and accumulated time with LDR24 ≥ 1 hPa h^{-1} in January averaged at the maximum of interannual variation. The climatological means are 1.5 hPa d^{-1} and 2.3 days, respectively. Based on the time series of LDR24P1, we analyze the composites for the years in which LDR24P1 is larger (positive year, PY) and smaller (negative year, NY) than the climatology. The differences between the PY and NY composites show that the positive wind stress curl and LDR24P1 are larger in PY than in NY (Figures 5b and 5c).

The monthly root-mean-square (RMS) of vertical velocity based on 3 day interval data, which is the average amplitude of the vertical velocity, shows significant responses to the interannual variability of the explosive cyclone activity. The vertical velocity RMS increases southwest of the positive LDR24P1 anomaly (Figure 5b) and the response extends to depths near the bottom (Figures 6a and 6c). In particular, the

response is larger than approximately 2 m d^{-1} at depths below 3000 m. The temperature standard deviation from the monthly mean also shows a significant difference, although the response is limited to narrow regions. The significant temperature response has two peaks along 32°N and 39°N latitude (Figures 6b and 6d). The response distribution of the temperature deviation reflects the structures of thermoclines and western boundary currents. The significant zones appear over strong thermoclines between the zonal current maxima (Figure 6d). The results may indicate that the vertical mixing by oceanic eddies is more dominant than the explosive cyclone wind forcing along the Kuroshio Extension and the Oyashio.

6. Conclusions and Discussion

The impact of explosive cyclones on the North Pacific Ocean is investigated in the present study using long-term simulation data of an eddy-resolving OGCM. The cyclonic wind stress caused by explosive cyclones induces horizontal divergence within the ocean-mixed layer and upward flow in the deep ocean, and the upward flow then causes vertical advection and induces ocean cooling. In addition, the interannual variation of the explosive cyclone activity modifies the amplitudes of the vertical velocity and the submonthly scale temperature variation.

The analyzed simulation is forced by the daily mean wind stress with 2.5° horizontal resolutions. Higher resolutions of both time and space are required to reproduce a more realistic ocean response [*Furuichi et al*., 2008; *Komori et al*., 2008; *Jochum et al*., 2013; *Rimac et al*., 2013] as well as the dependence of the wind stress on the ocean surface velocity [*Rath et al*., 2013]. However, the physical shortcomings in the present simulation suggest that the realistic impact of explosive cyclones may be larger than the obtained results. Indeed, a test simulation forced by 6-hourly Japanese 25 year reanalysis with 1.25° horizontal resolutions (JRA-25 [*Onogi et al*., 2007]) shows similar oceanic response, but the amplitude is twice larger than that in the NCEP/NCAR simulation (Figure S1 in the supporting information).

The results of the present study suggest that explosive cyclone activity can modify the vertical mixing of the deep ocean. The reproducibility of explosive cyclones varies according to the climate models used in Coupled Model Intercomparison Project Phase 5 [*Seiler and Zwiers*, 2016], and uncertainty is introduced because the explosive cyclone tracks and strengths are modified by fine-scale SST distributions associated with mesoscale oceanic eddies and western boundary currents, such as the Kuroshio, the Oyashio, and the Gulf Stream, which are not represented well in most of the ocean components of climate models [*Nakamura et al*., 2012; *Iizuka et al*., 2013; *Hirata et al*., 2015]. Additionally, the horizontal resolution of the atmospheric component in the climate model is too coarse to represent explosive cyclones [*Willison et al*., 2013].

The interannual variability of explosive cyclone activity should be considered when estimating the energy budget of the NIW using OGCMs. To better understand the oceanic response to explosive cyclones, future investigations must include high-frequency outputs (shorter than 1 day) obtained from atmospheric-ocean coupled models in which oceanic eddies are resolved in the atmosphere and the ocean as well as high-frequency observations (less than 1 day) of the effect of explosive cyclones on all layers of the ocean.

Acknowledgments
This study is supported by the Japan Society for the Promotion of Science (JSPS), KAKENHI, under grant 26707025, 25242038, 16 K12591, and 16H01846. The authors gratefully acknowledge their discussions with Yuki Tanaka. The OFES simulation was conducted on the Earth Simulator under the support of the Japan Agency for Marine-Earth Science and Technology (JAMSTEC). The OFES data are available from JAMSTEC Data Catalog (http://www.godac.jamstec.go.jp/catalog/data_catalog/metadataDisp/JAMSTEC_OFES?lang=en).

References

Alford, M. H., J. A. MacKinnon, H. L. Simmons, and J. D. Nash (2016), Near-Inertial internal gravity waves in the ocean, *Annu. Rev. Mar. Sci.*, *8*, 150902153948007, doi:10.1146/annurev-marine-010814-015746.

Dippe, T., X. Zhai, R. J. Greatbatch, and W. Rath (2015), Interannual variability of wind power input to near-inertial motions in the North Atlantic, *Ocean Dyn.*, *65*, 859–875, doi:10.1007/s10236-015-0834-x.

Furuichi, N., T. Hibiya, and Y. Niwa (2008), Model-predicted distribution of wind-induced internal wave energy in the world's oceans, *J. Geophys. Res. Ocean*, *113*, C09034, doi:10.1029/2008JC004768.

Gyakum, J. R., J. R. Anderson, R. H. Grumm, and E. L. Gruner (1989), North Pacific cold-season surface cyclone activity: 1975–1983, *Mon. Weather Rev.*, *117*, 1141–1155, doi:10.1175/1520-0493(1989)117<1141:NPCSSC>2.0.CO;2.

Hirata, H., R. Kawamura, M. Kato, and T. Shinoda (2015), Influential role of moisture supply from the Kuroshio/Kuroshio extension in the rapid development of an extratropical cyclone, *Mon. Weather Rev.*, *143*, 4126–4144, doi:10.1175/MWR-D-15-0016.1.

Iizuka, S., M. Shiota, R. Kawamura, and H. Hatsushika (2013), Influence of the monsoon variability and sea surface temperature front on the explosive cyclone activity in the vicinity of Japan during Northern winter, *SOLA*, *9*, 1–4, doi:10.2151/sola.2013-001.

Jochum, M., B. P. Briegleb, G. Danabasoglu, W. G. Large, N. J. Norton, S. R. Jayne, M. H. Alford, and F. O. Bryan (2013), The impact of oceanic near-inertial waves on climate, *J. Clim.*, *26*, 2833–2844, doi:10.1175/JCLI-D-12-00181.1.

Kalnay, E., et al. (1996), The NCEP/NCAR 40-year reanalysis project, *Bull. Am. Meteorol. Soc.*, *77*, 437–471.

Komori, N., W. Ohfuchi, B. Taguchi, H. Sasaki, and P. Klein (2008), Deep ocean inertia-gravity waves simulated in a high-resolution global coupled atmosphere-ocean GCM, *Geophys. Res. Lett.*, *35*, L04610, doi:10.1029/2007GL032807.

Kuwano-Yoshida, A. (2014), Using the local deepening rate to indicate extratropical cyclone activity, *SOLA*, *10*, 199–203, doi:10.2151/sola.2014-042.

Kuwano-Yoshida, A., and S. Minobe (2016), Storm track response to SST fronts in the Northwestern Pacific region in an AGCM, *J. Clim.*, doi:10.1175/JCLI-D-16-0331.1 in press.

Masumoto, Y., et al. (2004), A fifty-year eddy-resolving simulation of the world ocean: preliminary outcomes of OFES (OGCM for the earth simulator), *J. Earth Simulator*, *1*, 35–56.

Minobe, S., A. Kuwano-Yoshida, N. Komori, S.-P. Xie, and R. J. Small (2008), Influence of the gulf stream on the troposphere, *Nature*, *452*, 206–209, doi:10.1038/nature06690.

Nakamura, H., T. Sampe, Y. Tanimoto, and A. Shimpo (2004), Observed associations among storm tracks, jet streams and midlatitude oceanic fronts, in *Earth's Climate: The Ocean-Atmosphere Interaction*, pp. 329–345, AGU, Washington, D. C.

Nakamura, H., A. Nishina, and S. Minobe (2012), Response of storm tracks to bimodal Kuroshio path states south of Japan, *J. Clim.*, *25*, 7772–7779, doi:10.1175/JCLI-D-12-00326.1.

Rath, W., R. J. Greatbatch, and X. Zhai (2013), Reduction of near-inertial energy through the dependence of wind stress on the ocean-surface velocity, *J. Geophys. Res. Ocean*, *118*, 2761–2773, doi:10.1002/jgrc.20198.

Ren, X., W. Perrie, Z. Long, and J. Gyakum (2004), Atmosphere–ocean coupled dynamics of cyclones in the midlatitudes, *Mon. Weather Rev.*, *132*, 2432–2451, doi:10.1175/1520-0493(2004)132<2432:ACDOCI>2.0.CO;2.

Rimac, A., J. S. Von Storch, C. Eden, and H. Haak (2013), The influence of high-resolution wind stress field on the power input to near-inertial motions in the ocean, *Geophys. Res. Lett.*, *40*, 4882–4886, doi:10.1002/grl.50929.

Rosati, A., and K. Miyakoda (1988), A general circulation model for upper ocean simulation, *J. Phys. Oceanogr.*, *18*, 1601–1626, doi:10.1175/1520-0485(1988)018<1601:AGCMFU>2.0.CO;2.

Onogi, K., et al. (2007), The JRA-25 reanalysis, *J. Meteorol. Soc. Jpn*, *85*, 369–432.

Sanders, F., and J. Gyakum (1980), Synoptic-dynamic climatology of the "bomb", *Mon. Weather Rev.*, *108*, 1589–1606, doi:10.1175/1520-0493(1980)108<1589:SDCOT>2.0.CO;2.

Sasaki, H., M. Nonaka, Y. Masumoto, Y. Sasai, H. Uehara, and H. Sakuma (2008), An eddy-resolving hindcast simulation of the quasiglobal ocean from 1950 to 2003 on the earth simulator, in *High Resolution Numerical Modelling of the Atmosphere and Ocean*, edited by K. Hamilton and W. Ohfuchi, chap. 10, pp. 157–185, doi:10.1007/978-0-387-49791-4_10.

Seiler, C., and F. W. Zwiers (2016), How well do CMIP5 climate models reproduce explosive cyclones in the extratropics of the Northern Hemisphere?, *Clim. Dyn.*, *46*, 1241–1256, doi:10.1007/s00382-015-2642-x.

Tanaka, Y., T. Hibiya, and H. Sasaki (2015), Downward lee wave radiation from tropical instability waves in the central equatorial Pacific Ocean: A possible energy pathway to turbulent mixing, *J. Geophys. Res. Ocean*, *120*, 7137–7149, doi:10.1002/2015JC011017.

Willison, J., W. A. Robinson, and G. M. Lackmann (2013), The importance of resolving mesoscale latent heating in the North Atlantic storm track, *J. Atmos. Sci.*, *70*, 2234–2250, doi:10.1175/JAS-D-12-0226.1.

Yao, Y., W. Perrie, W. Zhang, and J. Jiang (2008), Characteristics of atmosphere-ocean interactions along North Atlantic extratropical storm tracks, *J. Geophys. Res.*, *113*, D14124, doi:10.1029/2007JD008854.

Yoshida, A., and Y. Asuma (2004), Structures and environment of explosively developing extratropical cyclones in the northwestern pacific region, *Mon. Weather Rev.*, *132*, 1121–1142.